Biosensors and Bioelectronics 141 (2019) 111438

Contents lists available at ScienceDirect

Biosensors and Bioelectronics

journal homepage: www.elsevier.com/locate/bios

# A label-free and signal-on electrochemiluminescence strategy for sensitive amyloid-beta assay

Haixin Qin, Xue Gao, Xiaoyan Yang*, Wei Cao, Shufeng Liu**

*Key Laboratory of Optic-electric Sensing and Analytical Chemistry for Life Science, MOE, Shandong Key Laboratory of Biochemical Analysis, Key Laboratory of Analytical Chemistry for Life Science in Universities of Shandong, College of Chemistry and Molecular Engineering. Qingdao University of Science and Technology, Qingdao, 266042, PR China*

ARTICLE INFO

*Keywords:*
Electrochemiluminescence
Amyloid-beta
Label-free
Signal-on
Luminol

ABSTRACT

Development of a simple, cost-effective and sensitive biosensing strategy is highly desirable to advance the applications in Alzheimer's disease diagnosis. In this paper, we present a simple, label-free and signal-on electrochemiluminescence (ECL) aptasensor for the detection of amyloid-beta (Aβ) peptide using luminol as ECL emitter and in-situ generated reactive oxygen species (ROS) as coreactant via catalytic reaction between $Cu^{2+}$-Aβ and the dissolved $O_2$ in the presence of ascorbic acid (AA). $Aβ_{16}$, the binding site of $Cu^{2+}$ in the monomeric full-length Aβ, was used as a model in present study. As a result, this signal-on ECL aptasensor has exhibited favorable analytical performance for $Aβ_{16}$ monomer with a linear range of $1.0 \times 10^{-13}$ mol/L-$1.0 \times 10^{-8}$ mol/L and a limit of detection of $3.5 \times 10^{-14}$ mol/L (S/N = 3). Furthermore, the proposed biosensor was also able to detect the full length $Aβ_{40}$ not only in the phosphate buffer saline (PBS) solution but also in human serum. The presented biosensor represents a promising, simple, turn-on and label-free diagnostic tool for blood analysis.

## 1. Introduction

Alzheimer's disease (AD), which is the most prevalent neurodegenerative disease, is characterized by progressive and irreversible impairment of memory, communication skills, and cognitive ability (Lee et al., 2019). With the advent of the aging population, AD has been a major public health concern in many countries. The etiology of AD has been suggested to be correlated with the aggregation of amyloid-β (Aβ) peptides in different parts of the brain (Hardy and Selkoe, 2002; Choi et al., 2017). Aβ peptides, consisting of 39–43 amino acid residues, are derived from the amyloid precursor protein through sequential cleavage by β-secretase and γ-secretase (Ghasemi et al., 2018). 40-residue $Aβ_{40}$ and 42-residue $Aβ_{42}$ are the most common forms of Aβ, which are considered as well-established and internationally validated biomarkers for early diagnosis of AD (Selkoe, 2004; Humpel, 2011). Particularly, $Aβ_{40}$ presents in larger amounts in the brain. $Aβ_{42}$ is more neurotoxic and has a higher tendency to aggregate (Sharma et al., 2012.). It has also been shown that redox active metal, such as $Zn^{2+}$, $Cu^{2+}$ and $Fe^{3+}$, are responsible for the aggregation of the Aβ peptides since they could be found at much higher concentrations in the neocortex of the brain (Bush, 2003). In order to gain insight into the role of metal ions in AD, the coordination of metal ions, especially $Cu^{2+}$, to Aβ has been widely studied. Though the process of $Cu^{2+}$ induced Aβ deposition is still questionable, it plays a significant role in the generation of neurotoxic reactive oxygen species (ROS) and oxidative stress (Pramanik et al., 2011). $Cu^{2+}$-Aβ could catalyze the reduction of $O_2$ to $H_2O_2$ in the presence of biological reducing agents (e.g., ascorbate), which finally leads to neuronal cells death (Reybier et al., 2016; Alies et al., 2011). The aggregation morphology of an amyloid peptide contains a monomer, oligomer, protofibril and mature fibril. Aβ oligomers are now considered to be more toxic than the senile plaques via various events including the production of ROS (Alies et al., 2013). Multiple analytical approaches, such as enzyme-linked immunosorbent assay (Klaver et al., 2010; Yang et al., 2013), fluorescence (Alies et al., 2014; Takahashi and Miharab, 2012; Liu et al., 2018; Zhu et al., 2016), surface plasmon resonance (Yi et al., 2016), colorimetry (Zhu et al., 2018; Deng et al., 2018), electrochemical impedance spectroscopy (Rushworth et al., 2014), and ECL (Ke et al., 2018) have been developed for the detection of Aβ monomers or oligomers in the diagnosis of AD.

ECL is an attractive analytical technique due to its high detection sensitivity, simple instrumentation and wide linear range. Tris (2,2′-bipyridyl) ruthenium (II) (Yuan et al., 2006; Wang et al., 2016; Zhang et al., 2018), luminol (Qiao et al., 2018; Li et al., 2018; Huo et al.,

* Corresponding author.
** Corresponding author.
*E-mail addresses:* xyang@qust.edu.cn (X. Yang), sliu@qust.edu.cn (S. Liu).

https://doi.org/10.1016/j.bios.2019.111438
Received 28 March 2019; Received in revised form 10 June 2019; Accepted 12 June 2019
Available online 24 June 2019
0956-5663/ 

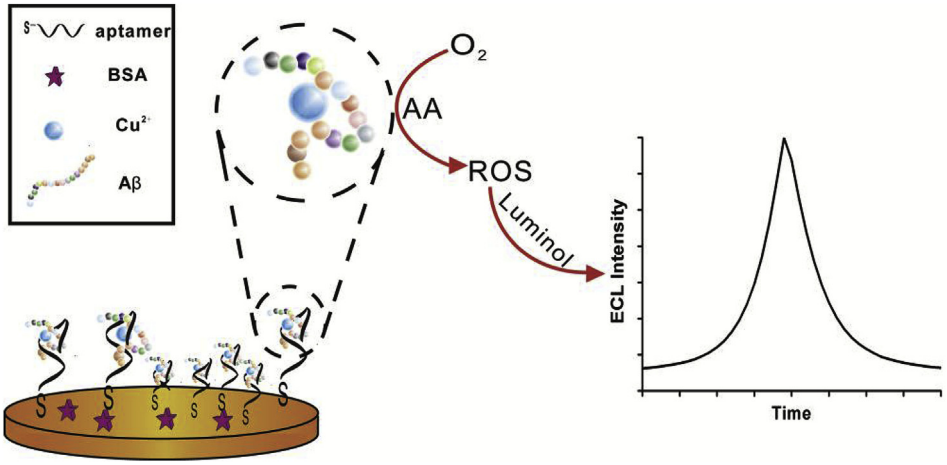


**Scheme 1.** Scheme illustration of the luminol ECL enhancing mechanism based on in situ generation of ROS accelerated by $Cu^{2+}$-Aβ complexes.

2018), metal nanoclusters (Zhou et al., 2017; Zhai et al., 2017), carbon nitride (Sha et al., 2019; Zhou et al., 2016), and semiconductor quantum dots (Liu et al., 2014 ; Jiang and Wang, 2014) have been widely served as ECL emitters for analytical application. Among these ECL emitters, luminol-based ECL system has been applied in the fabrication of the biosensors for the detection of the biomarkers. It is a well-known system to produce strong ECL emission at a low anode potential using $H_2O_2$ as coreactant (Khoshfetrat et al., 2015; Gu et al., 2015). In this work, we present a simple, label-free and signal-on ECL aptasensor for specific detection of Aβ peptide using luminol as ECL emitter and in-situ generated ROS as coreactant via catalytic reaction between $Cu^{2+}$-Aβ and the dissolved $O_2$ in the presence of AA. Aptamers are a prominent class of synthetic short single-stranded DNA or RNA oligonucleotide sequences that can bind to their targets with high affinity and specificity (Famulok et al., 2007). Aptamers can potentially target the pathogenic components of Alzheimer's disease (Tannenberg et al., 2013). As illustrated in Scheme 1, the aptamer, which was covalently immobilized on gold electrode via the Au–S bond, was used as the probe DNA to bind target Aβ peptide. Target Aβ peptide was coordinated with $Cu^{2+}$ to form $Cu^{2+}$-Aβ complexes and then the complexes could be recognized by the aptamers immobilized on the electrode. Luminol could generate a strong ECL signal with the assistance of ROS, which was generated in situ via a catalytic reaction between $Cu^{2+}$-Aβ-aptamers and the dissolved $O_2$ in the presence of AA. The full-length peptide ($Aβ_{40}$) and C-terminal truncated version ($Aβ_{16}$) can both bind to $Cu^{2+}$ with a high affinity in the same coordinating environment. However, unlike $Aβ_{40}$, $Aβ_{16}$ does not fibrillize, making it a useful model for studying the coordination of Aβ with $Cu^{2+}$ (Karr and Szalai, 2007). Therefore, the $Aβ_{16}$ peptide which represents the minimum Aβ sequence involved in $Cu^{2+}$ binding was used as a model in the present study. As a result, this signal-on ECL aptasensor has exhibited favorable analytical performance for the detection of $Aβ_{16}$ monomer. Furthermore, the proposed aptasensor was also able to detect the full length of $Aβ_{40}$ not only in the PBS solution but also in human serum.

## 2. Experimental section

### 2.1. Chemicals and reagents

All materials used were of analytical grade. Luminol and Tris (2-carboxyethyl) phosphine (TCEP) were obtained from Aladdin. $Aβ_{16}$, $Aβ_{40}$ and Aβ-targeting aptamer were purchased from Shanghai Sangon Biotechnology (Shanghai, China) and contained the following sequences: 5′–HS–GCC TGT GGT GTT GGG GCG GGT GCG-3′ (Aβ-targeting aptamer), DAEFRHDSGYEVHHQK ($Aβ_{16}$) and DAEFRHDSGYEVHHQKLVFFAEDVGSNKGAILGLMVGGVV($Aβ_{40}$). Carcinoem

- bryonic antigen (CEA), Bovine serum albumin (BSA) and alpha fetoprotein (AFP) were obtained from BIOCELL. NaCl, KCl, $NaH_2PO_4$, $Na_2HPO_4$, $CuSO_4$ were bought from BoDi (TianJin, China). L-Ascorbic Acid (AA) was acquired from Energy Chemical (Shanghai, China).

### 2.2. Apparatus

ECL were carried out on a model MPI-E ECL system (Xi'an Remex Electronics Co. Ltd., Xi' an, China). Electrochemical impedance spectroscopy (EIS) was collected on a CHI 660E electrochemical workstation (Chenhua, Shanghai, China) in 1.0 M KCl containing 5.0 mM $[Fe(CN)_6]^{3-/4-}$. The bare or modified gold working electrode, Ag/AgCl (saturated KCl) reference electrode, and platinum counter electrode were used for electrochemical and ECL measurements. Transmission electron microscopy (TEM) of the different forms of Aβ was performed using a JEM-F200 TEM instrument (Hitachi, japan).

### 2.3. Preparation of the aptamers modified gold electrode

The gold electrodes were first polished with 0.3 and 0.05 μm alumina powder and then sonicated in ultrapure water, ethanol and ultrapure water sequentially for 3 min and dried under nitrogen. Finally, the well-polished electrode was subjected to electrochemical pretreatment by cycling the potential between -0.3 V and 1.5 V in $H_2SO_4$ (0.5 M) at scan rate 100 mV $s^{-1}$ until a stable cyclic voltammogram was obtained. Afterwards, cleaned gold electrodes were soaked in the 10 μM aptamer solution for 6 h in 37 °C. Prior to immobilization, the disulfide bond of DNA was reduced with 10 mM TCEP for 1 h. Finally, the aptamer modified gold electrodes were incubated with BSA solution (1%, w/v) for 1 h to block nonspecific sites. After this step, the modified electrodes were washed with PBS buffer and placed under 4 °C for used.

### 2.4. Preparation of the Aβ-$Cu^{2+}$ complexes

Lyophilized peptides were dissolved in phosphate buffer (0.1 M, pH 7.4) to form Aβ monomer solution. For preparing Aβ-$Cu^{2+}$ complexes, Aβ monomer solution was incubated with $CuSO_4$ solution at the same concentration for 2 h at 37 °C. During the optimization of experimental parameters, the concentration of Aβ monomer solution and $CuSO_4$ solution was $1.0 \times 10^{-8}$ mol/L.

### 2.5. Measurement procedure

For ECL measurements, the aptamers modified gold electrodes were incubated with different concentrations of Aβ-$Cu^{2+}$ complexes at 37 °C for 2 h in 0.1 M PBS buffer (pH 7.4). Afterwards, the resulting electrode was washed with PBS buffer and then placed in the ECL cell. Finally, the ECL signal was detected in air-saturated PBS buffer containing 0.1 mM luminol solution and 0.1 mM AA solution. The ECL signals were carried out under cyclic voltammetry when the electrode potential was scanned from 0 V to 0.5 V at a scan of 100 mV $s^{-1}$. The voltage of PMT was set at 600 V in the process of detection.

### 2.6. Determination of $A\beta_{40}$ in human serum

The whole blood samples were collected from health volunteers in Qingdao Eight People's Hospital and centrifugated with low speed (5000 rpm) for 15 min to remove hemocytes. Then, the serum samples were transferred into centrifuge tube and stored at -20 °C before use. A series of serum samples containing different concentration of $A\beta_{40}$-$Cu^{2+}$ complexes were prepared by adding different concentration of $A\beta_{40}$ monomers and $Cu^{2+}$ at a molar ratio of 1:1. Then the serum samples were analyzed by aptasensor.

## 3. Results and discussion

### 3.1. Analysis of the feasibility of ECL aptasensor

It has been well revealed that $Cu^{2+}$ bind to the first 16 amino acid residues, and thus the C-terminally truncated $A\beta_{16}$ peptide is widely accepted as a valuable model of copper binding to monomeric $A\beta_{40}$ or $A\beta_{42}$ (Alies et al., 2012). However, screened DNA aptamers and their ability to capture AD biomarkers were specific to $A\beta_{40}$ or $A\beta_{42}$ in the previous literature (Shui et al., 2018). Since EIS has proved to have a sensitive insight on the change in surface features of the modified electrode, we used this technique to evaluate the binding affinity of the selected aptamers for $A\beta_{16}$ at first. In order to avoid the nonspecific adsorption, we utilized BSA solution as a blocker after the selected aptamer was modified onto gold electrodes. The diameter of semicircle in higher frequency range of Nyquist plots indicates the charge-transfer resistance ($R_{ct}$) at the electrode interface. As shown in Fig. 1A, the bare gold electrode exhibited almost a straight line of the impedance spectra, which was the characteristic of a diffusion-controlled electrochemical process (Fig. 1A, curve a). The immobilization of aptamers on the electrode induced an increased $R_{ct}$, which could be attributed to the diffusion inhibition of $[Fe(CN)_6]^{3-/4-}$ to the electrode surface by the introduced negatively charged phosphate backbone of the aptamers (Fig. 1A, curve b). The $R_{ct}$ increased further after the post-treatment with BSA, which was due to the non-specifically adsorbed BSA molecules offering an additional steric hindrance for the diffusion of the $[Fe(CN)_6]^{3-/4-}$ to the electrode surface (Fig. 1A, curve c). After incubation with $A\beta_{16}$ peptide, a significantly increased $R_{ct}$ was obtained (Fig. 1A, curve d), attributing to the formed $A\beta_{16}$-aptamer complex on the electrode surface, which offers an additional insulating layer of peptides to inhibit the interfacial electron transfer (Szymańska et al., 2007). However, when the aptamer was incubated with the Aβ-$Cu^{2+}$ complex, the $R_{ct}$ was lower than that of the $A\beta_{16}$-aptamer complex, which indicated a lower charge transfer resistance at the electrode interface (Fig. 1A, curve e). The decrease in the semicircle diameter maybe result from the positively charged $Cu^{2+}$ of the Aβ-$Cu^{2+}$ complex accelerating the diffusion of $[Fe(CN)_6]^{3-/4-}$ redox probe toward electrode surface. These results not only indicated that the selected aptamers had the capability to bind with $A\beta_{16}$ but also revealed the aptasensor was successfully fabricated.

ECL measurements were also conducted to follow the assembly process of the modified electrode and verify the detection feasibility for $A\beta_{16}$. The bare gold electrode showed a relatively weak ECL signal in air-saturated PBS solution containing luminol and AA (curve a in Fig. 1B). After aptamer was assembled and BSA was blocked on the electrode, the ECL intensity was only slightly higher or lower than that of bare electrode (curve b and c in Fig. 1B). After recognition of aptamer with Aβ peptides, an obvious increase of ECL intensity could be observed (curve d in Fig. 1B), indicating that the bound Aβ peptides can promote the ECL of luminol to some extent (Park et al., 2008; Du et al., 2014). Furthermore, the ECL signals of luminol for the Aβ-$Cu^{2+}$ complexes were further distinctly amplified (curve e in Fig. 1B). This also indicated that the complexes of $A\beta_{16}$ peptide with $Cu^{2+}$ could be well recognized by the immobilized aptamer on the electrode for catalyzing ECL of luminol. The ECL intensity for the recognized Aβ-$Cu^{2+}$ complexes was about three times higher than that of no target $A\beta_{16}$ peptide, suggesting the detection feasibility of the fabricated biosensor for Aβ peptides. The ECL mechanism of luminol catalyzed by Aβ-$Cu^{2+}$ complexes could be explained that the Aβ-$Cu^{2+}$ complexes could catalyze the dissolved $O_2$ to generate $H_2O_2$ and more reactive oxygen species, which then accelerated the formation of the excited luminol for emission enhancement of luminol (Zhang et al., 2014; Zuo et al., 2018). To further verify the ECL mechanism, the ECL responses of luminol in air-moved aqueous solution were also conducted. It was found that the ECL intensity was almost negligible (curve f in Fig. 1B), indicating the catalytic role of Aβ-$Cu^{2+}$ complexes toward the dissolved $O_2$ for luminol ECL enhancement.

The ECL spectrum in the presence of Aβ-$Cu^{2+}$ complexes was measured by a series of optical filters. As shown in Fig. 1C, the maximum emission of ECL was located at the peak of 460 nm, corresponding to the emission of 3-aminophthalate, which indicated ECL emission was originated from the electrochemical oxidation of luminol on the aptamer-modified gold electrode (Zhao et al., 2017). These

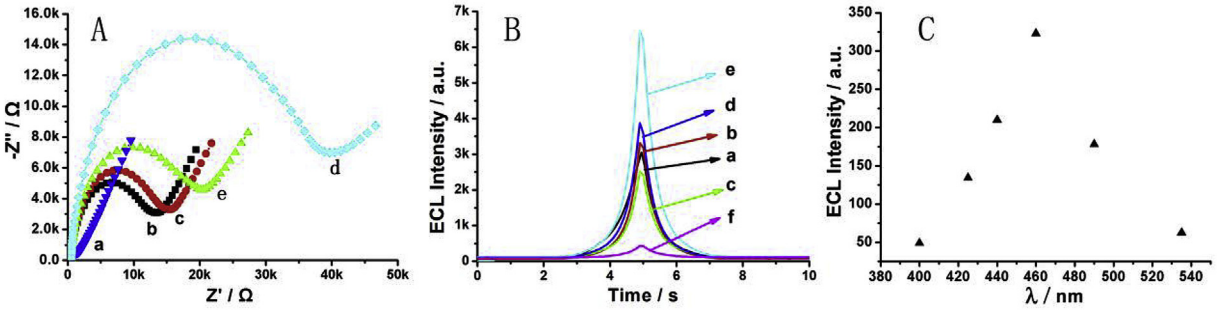


**Fig. 1.** (A) EIS responses of (a) bare electrode, (b) aptamers/electrode (c) aptamers/BSA/electrode, (d) $A\beta_{16}$/aptamers/BSA/electrode, (e) $Cu^{2+}$-$A\beta_{16}$/aptamers/BSA/electrode in 0.1 mM PBS containing 5.0 mM $[Fe(CN)_6]^{3-/4-}$ and 1.0 M KCl as the supporting electrolyte. (B) ECL intensity of (a) bare electrode, (b) aptamers/electrode (c) aptamers/BSA/electrode, (d) $A\beta_{16}$/aptamers/BSA/electrode, (e) $Cu^{2+}$-$A\beta_{16}$/aptamer/BSA/electrode in 0.1 M PBS solution (pH 7.4) containing 0.1 mM luminol solution and 0.1 mM AA, (f) $Cu^{2+}$-$A\beta_{16}$/aptamer/BSA/electrode in 0.1 M air-moved PBS buffer (pH 7.4) containing 0.1 mM luminol solution and 0.1 mM AA solution. (C) ECL spectrum of $Cu^{2+}$-$A\beta_{16}$/aptamers/BSA/GE in 0.1 M PBS buffer (pH 7.4) containing 0.1 mM luminol solution and 0.1 mM AA solution.

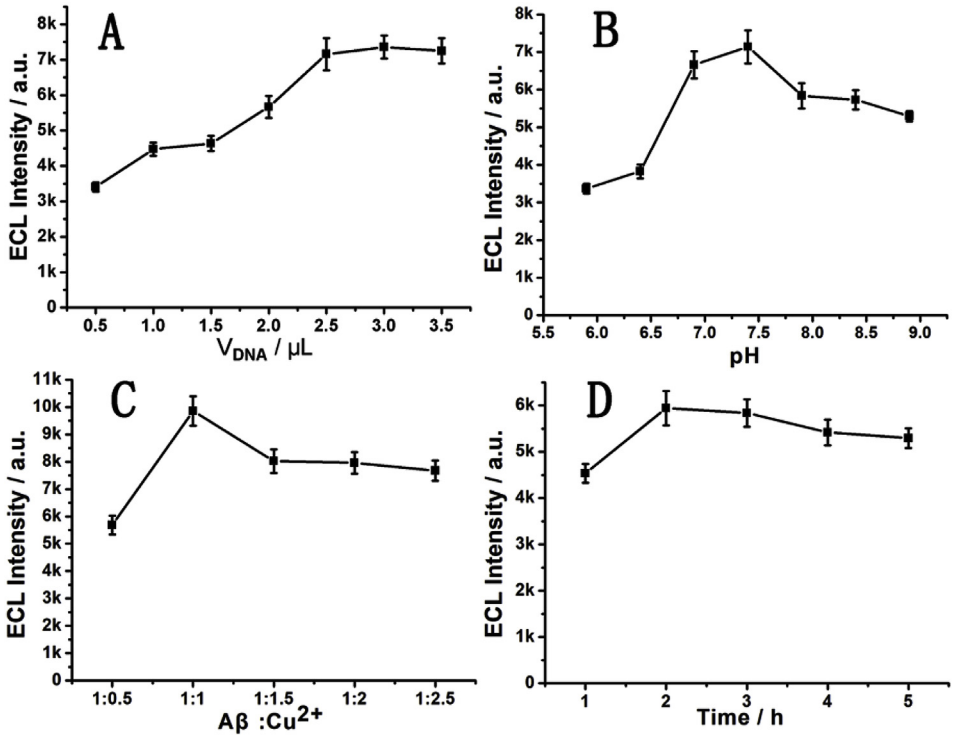


**Fig. 2.** (A) Optimization of the volume of the bound aptamer, (B) the pH dependence of $Cu^{2+}$ binding to $A\beta_{16}$ , (C) the effect of the molar ratio of Aβ to $Cu^{2+}$ on the ECL signal, (D) the effect of incubate time to obtain the Aβ-$Cu^{2+}$ complexes.

events may explain that the interaction of Aβ with redox-active $Cu^{2+}$ can lead to the formation of ROS (such as $H_2O_2$) (Parthasarathy et al., 2011).

### 3.2. Optimization of experimental parameters

To achieve excellent performances of the ECL biosensor, the experimental parameters are optimized. Firstly, the volume used for the immobilization of aptamer was investigated (Fig. 2A). The ECL intensity increased gradually with an increase of aptamer volume and tended to be stable when the volume of aptamer reached 2.5 μL. Thus, 2.5 μL of aptamer was used for the ECL biosensor fabrication throughout this work. Recent studies indicate that the coordination environment of $Cu^{2+}$ in soluble $Cu^{2+}$-Aβ complexes is highly sensitive to pH (Alies et al., 2011). Therefore, the pH dependence for the $Cu^{2+}$ binding to $A\beta_{16}$ was investigated. Fig. 2B displayed the effect of buffer solution pH on the ECL intensity. The ECL intensity increased with the increase of pH and then reached a maximum at pH 7.4. $A\beta_{16}$, a hydrophilic portion of an extracellular domain of Aβ, is able to form hydrogen bonds with surrounding water molecules to stabilize the structure of the PPII helix at pH 7.4 (Stapley and Creamer, 1999; Adzhubei and Sternberg, 1993). In the presence of $Cu^{2+}$, $A\beta_{16}$ peptide fragment forms β-sheets since $Cu^{2+}$ may not only alter the structure of $A\beta_{16}$ by binding but also cause the peptide to undergo a conformational change from a helix to a β-sheet by displacing water molecules around the peptide backbone (Chen et al., 2006.). Therefore, pH 7.4 was chosen for this work. The aggregation state of Aβ peptide is also governed by the $Cu^{2+}$: peptide molar ratio (Smith et al., 2007). The ratio of Aβ to $Cu^{2+}$ on the ECL signal was further investigated. Fig. 2C demonstrates the ECL intensities at different molar ratios of $Cu^{2+}$ to Aβ. The ECL intensity increased with the increase of molar ratio of $Cu^{2+}$ to Aβ and then decreased with the further increase of molar ratio over 1:1. Hence, the molar ratio of 1:1 for the Aβ to $Cu^{2+}$ was used for biosensor fabrication. Moreover, the incubation time to obtain the Aβ-$Cu^{2+}$ complexes was studied and showed in Fig. 2D. As the incubation time increased, the ECL intensity increased and reached the maximum at 2h. As a result, 2 h of the incubation between Aβ peptide and $Cu^{2+}$ was selected as the optimized time.

### 3.3. Comparison of ECL responses with different $A\beta_{16}$ aggregates

To determine whether the proposed biosensor could monitor the aggregation of monomeric $A\beta_{16}$ peptides after binding with $Cu^{2+}$, the effect of various Aβ aggregation species on ECL responses were investigated. Four various Aβ-$Cu^{2+}$ complexes were obtained by incubating $A\beta_{16}$ monomer with $Cu^{2+}$ at 37 °C for 2 h, 5 h and 36 h, 72 h, respectively. As shown in Fig. 3A-D (inset), under the same conditions, the ECL intensity decreased with the increased incubation time, maybe owing to the Aβ aggregation reducing its binding with $Cu^{2+}$. We also examined the morphological changes of monomeric $A\beta_{16}$ peptides after binding with $Cu^{2+}$. Fig. 3A-D shows the TEM images of the above aggregates. In the first 2 h, the monomers aggregated and formed oligomeric species with average width of ~50 nm (Fig. 3A). And then oligomers become much bigger along with the incubation time (Fig. 3B-D). It has been proposed that the binding of $Cu^{2+}$ to Aβ monomers may affect the aggregation rate or type of Aβ (Atwood et al., 1998; Yoshiike et al., 2001). These observations were indicated indirectly that the conformational change of $A\beta_{16}$ peptide was induced by the bound $Cu^{2+}$ ions, implying the possibility of the proposed biosensor to monitor the aggregation process of monomeric $A\beta_{16}$ peptides.

### 3.4. Detection of $A\beta_{16}$ monomers by the fabricated ECL biosensor

Detection of the amyloid monomers is of great importance in the diagnosis of amyloidogenesis (Huang et al., 2017.). Under the optimized experimental conditions, the ECL responses of the immunosensor with different $A\beta_{16}$ monomers concentrations were detected. As shown in Fig. 4A. The intensity of ECL increased with the increase of $A\beta_{16}$ concentration. The corresponding calibration plot was presented in Fig. 4B, indicating that there was an excellent linear relationship

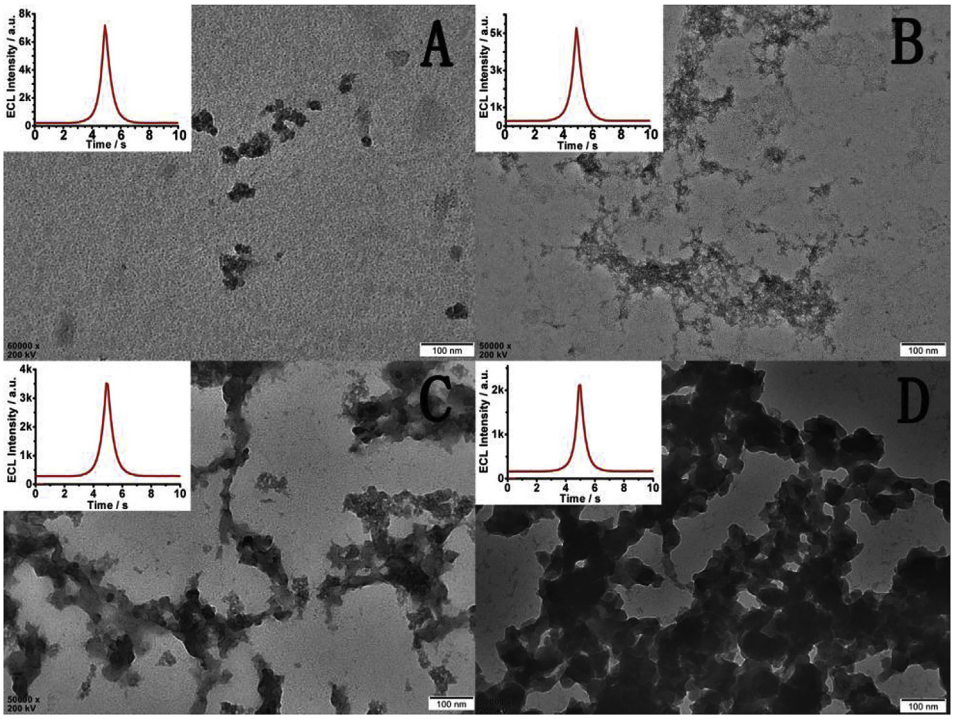


**Fig. 3.** TEM image of the morphological changes of monomeric $A\beta_{16}$ peptides after binding with $Cu^{2+}$ at (A) 2 h, (B) 5 h, (C) 36 h, (D) 72 h, respectively. Inset: Comparison of ECL responses in various Aβ aggregation species prepared by $A\beta_{16}$ monomer incubating with $Cu^{2+}$ for (A) 2 h, (B) 5 h, (C) 36 h, (D) 72 h, respectively.

between the ECL intensity and the $A\beta_{16}$ monomers concentrations from $1.0 \times 10^{-13}$ mol/L to $1.0 \times 10^{-8}$ mol/L and the limit of detection was as low as $3.5 \times 10^{-14}$ mol/L (S/N = 3). The results indicated that the fabricated ECL sensor could quantify Aβ peptide with high sensitivity. In addition, the analytical performance of the proposed ECL biosensor was compared with the previous reports (Table S1, See the Supplementary Materials). It was found that the proposed biosensor exhibited a more wide detection range than most of them, and had a relatively low detection limit.

### 3.5. Selectivity, reproducibility and stability of the ECL biosensor

To evaluate the selectivity of the proposed biosensor for quantitative analysis of Aβ peptide, some proteins with same concentration were selected as the interference, including BSA, CEA and thrombin. As shown in Fig. 5A, no remarkable signal was observed in comparison with that in the presence of $A\beta_{16}$ only. In the case of adding all the proteins, the ECL responses were strong and there was no obvious difference between $A\beta_{16}$ and the mixture. These results indicated the proposed biosensor had a high selectivity for the detection of Aβ peptide. The reproducibility of the proposed ECL sensor was also investigated with four electrodes in the same conditions. The proposed ECL biosensor showed an acceptable reproducibility with a relative standard deviation (RSD) of 5.05%.

Fig. 5B displays that ECL emission under 400 s of continuous potential scans between 0.0 V and 0.5 V (vs Ag/AgCl) in 0.1 M PBS at 100 mV $s^{-1}$. Stable and high ECL signals were observed, suggesting that the biosensor displayed a good stability for the determination of Aβ peptide.

### 3.6. Sensing of $A\beta_{40}$ in buffer solution and serum samples

The C-terminally truncated $A\beta_{16}$ has been preferred, especially when high concentrations are used as a valuable model of $Cu^{2+}$ binding site in the monomeric full-length Aβ. In the present study, the selective aptamer is against the full length $A\beta_{40}$, so the proposed biosensor should be applied to detect $A\beta_{40}$. The evidence as shown in Fig. S1 (See the Supplementary Materials) proved the argument. After the addition of $A\beta_{40}$-$Cu^{2+}$ complexes and incubation with the aptamer modified on the electrode, an extremely strong ECL signal could be detected,

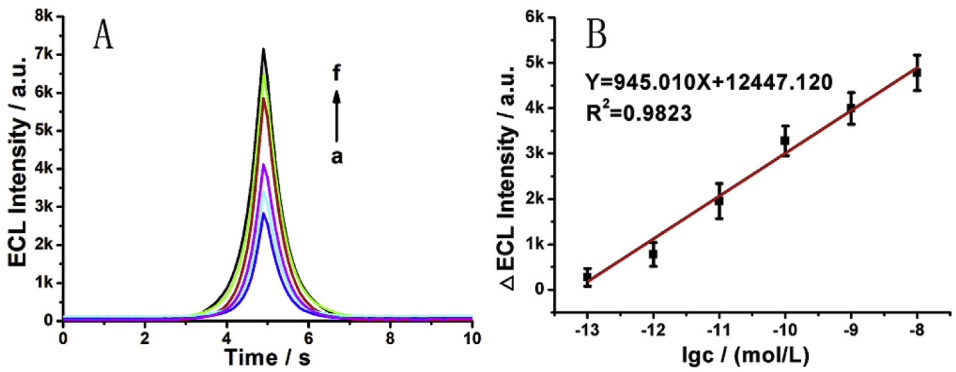


**Fig. 4.** (A) ECL intensity of the proposed ECL biosensor with different concentrations of $A\beta_{16}$: (a) $1.0 \times 10^{-13}$ mol/L; (b) $1.0 \times 10^{-12}$ mol/L; (c) $1.0 \times 10^{-11}$ mol/L; (d) $1.0 \times 10^{-10}$ mol/L; (e) $1.0 \times 10^{-9}$ mol/L; (f) $1.0 \times 10^{-8}$ mol/L. (B) Calibration curves of $A\beta_{16}$ determination.

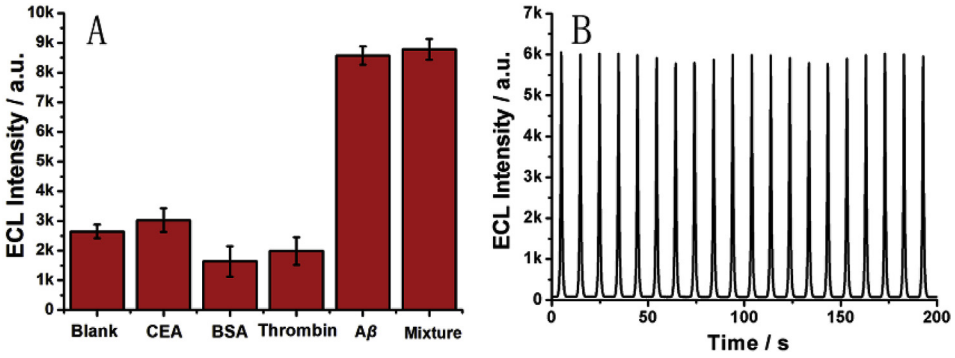


**Fig. 5.** (A) The selectivity of the proposed biosensor: blank (without Aβ), CEA ($1.0 \times 10^{-8}$ mol/L), BSA ($1.0 \times 10^{-8}$ mol/L), Thrombin ($1.0 \times 10^{-8}$ mol/L), Aβ ($1.0 \times 10^{-8}$ mol/L) and a mixture of CEA ($1.0 \times 10^{-8}$ mol/L), BSA ($1.0 \times 10^{-8}$ mol/L), Thrombin ($1.0 \times 10^{-8}$ mol/L), Aβ ($1.0 \times 10^{-8}$ mol/L). (B) The ECL stability of the proposed biosensor.

indicating that luminol could generate strong emission accelerated by in-situ generated ROS in the presence of $A\beta_{40}$-$Cu^{2+}$ complexes and AA.

$A\beta_{40}$ and $A\beta_{42}$ are chief components of the senile plaques in AD. However, the affinity between $A\beta_{42}$ and $Cu^{2+}$ is lower than that of $A\beta_{40}$ (Liu et al., 2018). Furthermore, the concentration of $A\beta_{42}$ is less than one-tenth of $A\beta_{40}$ in human fluid samples and senile plaque (Hamley, 2012). Therefore, $A\beta_{42}$ does not interfere the determination of $A\beta_{40}$ in real samples. The feasibility of the constructed ECL platform for the detection of $A\beta_{40}$ in real samples was also tested using the standard addition method. As show in Table S2 (See the Supplementary Materials), acceptable recoveries from 99.3% to 101.8% were obtained for Aβ in serum sample, illustrating the applicability of the proposed system for the diagnosis of AD.

## 4. Conclusions

In summary, a simple, label-free and signal-on ECL strategy was well proposed for sensitive and selective amyloid-beta assay, which took full advantages of the catalytic ability of $Cu^{2+}$-Aβ complexes toward the dissolved oxygen for enhancing the ECL of luminol. The proposed biosensor was also employed to follow the aggregation process of $A\beta_{16}$ monomer accelerated by $Cu^{2+}$ to some extent. The sensitive and selective detection toward $A\beta_{16}$ could be achieved with an attractive detection limit of $3.5 \times 10^{-14}$ mol/L. The developed ECL biosensor was also applicative for the analysis of Aβ in serum sample. Thus, the current study offers a promising avenue for ECL biosensor fabrication served for the applications in Alzheimer's disease diagnosis.

## Declaration of interests

The authors declare that they have no known competing financial interests or personal relationships that could have appeared to influence the work reported in this paper.

## CRediT authorship contribution statement

**Haixin Qin:** Methodology, Investigation, Writing - original draft. **Xue Gao:** Methodology, Visualization. **Xiaoyan Yang:** Conceptualization, Writing - review & editing, Supervision. **Wei Cao:** Software, Data curation, Formal analysis. **Shufeng Liu:** Validation, Data curation, Supervision.

## Acknowledgement

We appreciated the finance supports from the Natural Science Foundation of Shandong Province of China (JQ201704, ZR2019MB051), the Key Research and Development Project of Shandong Province (2018GGX102001), the National Natural Science Foundation of China (21475072, 21005044) and the Foundation of Key Laboratory of Optic-electric Sensing and Analytical Chemistry for Life Science, Qingdao University of Science and Technology (SATM201701).

## Appendix A. Supplementary data

Supplementary data to this article can be found online at https://doi.org/10.1016/j.bios.2019.111438.

## References

Adzhubei, A.A., Sternberg, M.J., 1993. J. Mol. Biol. 229, 472–493.
Alies, B., Eury, H., Bijani, C., Rechignat, L., Faller, P., Hureau, C., 2011. Inorg. Chem. 50, 11192–11201.
Alies, B., Bijani, C., Sayen, S., Guillon, E., Faller, P., Hureau, C., 2012. Inorg. Chem. 51, 12988–13000.
Alies, B., Renaglia, E., Rózga, M., Bal, W., Faller, P., Hureau, C., 2013. Anal. Chem. 85, 1501–1508.
Alies, B., Eury, H., Essassiel, M., Pratviel, G., Hureau, C., Faller, P., 2014. Anal. Chem. 86, 11877–11882.
Atwood, C.S., Moir, R.D., Huang, X., Scarpa, R.C., Bacarra, N.M.E., Romano, D.M., Hartshorn, M.A., Tanzi, R.E., Bush, A.I., 1998. J. Biol. Chem. 273, 12817–12826.
Bush, A.I., 2003. Trends Neurosci. 26, 207–214.
Chen, Y.R., Huang, H.B., Chyan, C.L., Shiao, M.S., Lin, T.H., Chen, Y.C., 2006. J. Biochem. 139, 733–740.
Choi, T.S., Lee, H.J., J. Han, Y., Lim, M.H., Kim, H.I., 2017. J. Am. Chem. Soc. 139, 15437–15445.
Deng, C., Liu, H., Zhang, M., Deng, H., Lei, C., Shen, L., Jiao, B., Tu, Q., Jin, Y., Xiang, L., Deng, W., Xie, Y., Xiang, J., 2018. Anal. Chem. 90, 1710–1717.
Du, X., Wang, Z., Zheng, Y., Li, H., Ni, J., Liu, Q., 2014. Inorg. Chem. 53, 1672–1678.
Famulok, M., Hartig, J.S., Mayer, G., 2007. Chem. Rev. 107, 3715–3743.
Ghasemi, F., Hormozi-Nezhad, M.R., Mahmoudi, M., 2018. Nanoscale 10, 6361–6368.
Gu, W., Deng, X., Gu, X., Jia, X., Lou, B., Zhang, X., Li, J., Wang, E., 2015. Anal. Chem. 87, 1876–1881.
Hamley, I.W., 2012. Chem. Rev. 112, 5147–5192.
Hardy, J., Selkoe, D.J., 2002. Science 297, 353–356.
Huang, H., Li, P., Zhang, M., Yu, Y., Huang, Y., Gu, H., Wang, C., Yang, Y., 2017. Nanoscale 9, 5044–5048.
Humpel, C., 2011. Trends Biotechnol. 29, 26–32.
Huo, X.-L., Zhang, N., Yang, H., Xu, J.-J., Chen, H.-Y., 2018. Anal. Chem. 90, 13723–13728.
Jiang, H., Wang, X., 2014. Anal. Chem. 86, 6872–6878.
Karr, J.W., Szalai, V.A., 2007. J. Am. Chem. Soc. 129, 3796–3797.
Ke, H., Sha, H., Wang, Y., Guo, W., Zhang, X., Wang, Z., Huang, C., Jia, N., 2018. Biosens. Bioelectron. 100, 266–273.
Khoshfetrat, S.M., Ranjbari, M., Shayan, M., Mehrgardi, M.A., Kiani, A., 2015. Anal. Chem. 87, 8123–8131.
Klaver, A.C., Patrias, L.M., Coffey, M.P., Finke, J.M., Loeffler, D.A., 2010. J. Neurosci. Methods 187, 263–269.
Lee, B., Chung, Y.J., Park, C.B., 2019. Biomaterials 190–191, 121–132.
Li, X., Lu, P., Wu, B., Wang, Y., Wang, H., Du, B., Pang, X., Wei, Q., 2018. Biosens. Bioelectron. 112, 40–47.
Liu, Y., Lei, J., Huang, Y., Ju, H., 2014. Anal. Chem. 86, 8735–8741.
Liu, B., Shen, H., Hao, Y., Zhu, X., Li, S., Huang, Y., Qu, P., Xu, M., 2018. Anal. Chem. 90, 12449–12455.
Park, L., Zhou, P., Pitstick, R., Capone, C., Anrather, J., Norris, E.,H., Younkin, L., Younkin, S., Carlson, G., McEwen, B.,S., Iadecola, C., 2008. Proc. Natl. Acad. Sci. Unit. States Am. 105, 1347–1352.
Parthasarathy, S., Long, F., Miller, Y., Xiao, Y., McElheny, D., Thurber, K., Ma, B., Nussinov, R., Ishii, Y., 2011. J. Am. Chem. Soc. 133, 3390–3400.
Pramanik, D., Ghosh, C., Dey, S.G., 2011. J. Am. Chem. Soc. 133, 15545–15552.
Qiao, Y., Li, Y., Fu, W., Guo, Z., Zheng, X., 2018. Anal. Chem. 90, 9629–9636.
Reybier, K., Ayala, S., Alies, B., Rodrigues, J.V., Rodriguez, S.B., Penna, G.L., Collin, F., Gomes, C.M., Hureau, C., Faller, P., 2016. Angew. Chem. Int. Ed. 55, 1085–1089.
Rushworth, J.V., Ahmed, A., Griffiths, H.H., Pollock, N.M., Hooper, N.M., Millner, P.A., 2014. Biosens. Bioelectron. 56, 83–90.

Selkoe, D.J., 2004. Nat. Cell Biol. 6, 1054–1061.
Sha, H., Zhang, Y., Wang, Y., Ke, H., Xiong, X., Jia, N., 2019. Biosens. Bioelectron. 124–125, 59–65.
Sharma, A.K., Pavlova, S.T., Kim, J., Finkelstein, D., Hawco, N.J., Rath, N.P., Kim, J., Mirica, L.M., 2012. J. Am. Chem. Soc. 134, 6625–6636.
Shui, B., Tao, D., Florea, A., Cheng, J., Zhao, Q., Gu, Y., Li, W., Jaffrezic-Renault, N., Mei, Y., Guo, Z., 2018. Biochimie 147, 13–24.
Smith, D.P., Ciccotosto, G.D., Tew, D.J., Fodero-Tavoletti, M.T., Johanssen, T., Masters, C.L., Barnham, K.J., Cappai, R., 2007. Biochem 46, 2881–2891.
Stapley, B.J., Creamer, T.P., 1999. Protein Sci. 8, 587–595.
Szymańska, I., Radecka, H., Radecki, J., Kaliszan, R., 2007. Biosens. Bioelectron. 22, 1955–1960.
Takahashi, T., Miharab, H., 2012. Chem. Commun. 48, 1568–1570.
Tannenberg, R.K., Lauridsen, L.H., Kanwar, J.R., Dodd, P.R., Veedu, R.N., 2013. Curr. Alzheimer Res. 10, 442–448.
Wang, H., Yuan, Y., Zhuo, Y., Chai, Y., Yuan, R., 2016. Anal. Chem. 88, 2258–2265.
Yang, T., Hong, S., O'Malley, T., Sperling, R.A., Walsh, D.M., Selkoea, D.J., 2013. Alzheimer's Dementia 99–112.
Yi, X., Feng, C., Hu, S., Li, H., Wang, J., 2016. Analyst 141, 331–336.
Yoshiike, Y., Tanemura, K., Murayama, O., Akagi, T., Murayama, M., Sato, S., Sun, X., Tanaka, N., Takashima, A., 2001. J. Biol. Chem. 276, 32293–32299.
Yuan, J., Li, T., Yin, X.B., Guo, L., Jiang, X., Jin, W., Yang, X., Wang, E., 2006. Anal. Chem. 78, 2934–2938.
Zhai, Q., Xing, H., Zhang, X., Li, J., Wang, E., 2017. Anal. Chem. 89, 7788–7794.
Zhang, H.R., Wu, M.S., Xu, J.J., Chen, H.Y., 2014. Anal. Chem. 86, 3834–3840.
Zhang, Y., Yang, H., Cui, K., Zhang, L., Xu, J., Liu, H., Yu, J., 2018. J. Mater. Chem. 6, 19611–19620.
Zhao, X., Zhou, W., Lu, C., 2017. Anal. Chem. 89, 10078–10084.
Zhou, Z., Shang, Q., Shen, Y., Zhang, L., Zhang, Y., Lv, Y., Li, Y., Liu, S., Zhang, Y., 2016. Anal. Chem. 88, 6004–6010.
Zhou, Y., Chen, M., Zhuo, Y., Chai, Y., Xu, W., Yuan, R., 2017. Anal. Chem. 89, 6787–6793.
Zhu, L., Zhang, J., Wang, F., Wang, Y., Lu, L., Feng, C., Xu, Z., Zhang, W., 2016. Biosens. Bioelectron. 78, 206–212.
Zhu, X., Zhang, N., Zhang, Y., Liu, B., Chang, Z., Zhou, Y., Hao, Y., Ye, B., Xu, M., 2018. Anal. Methods 10, 641–645.
Zuo, F., Zhang, H., Xie, J., Chen, S., Yuan, R., 2018. Electrochim. Acta 271, 173–179.